Understanding Freezing Behavior in Porous Materials

Ravi Radhakrishnan[1], Keith E. Gubbins[2],
Malgorzata Sliwinska-Bartkowiak[3] and Katsumi Kaneko[4]

[1] Department of Chemical Engineering, Massachusetts Institute of Technology, Cambridge, MA 02139, USA (E-mail: rradhak@mit.edu);
[2] Department of Chemical Engineering, North Carolina State University, Raleigh, NC 27695, USA (E-mail: keg@ncsu.edu);
[3] Institute of Physics, Adam Mickiewicz University, 61-614 Poznan, Poland (E-mail:msb@main.amu.edu.pl);
[4] Department of Chemistry, Chiba University, Chiba 263-8522, Japan (E-mail: kaneko@pchem2.chiba-u.ac.jp)

Abstract
Using molecular simulations and free energy calculations based on Landau theory, we show that the freezing/melting behavior of fluids of small molecules in pores of simple geometry can be understood in terms of two main parameters: the pore width H^* (expressed as a multiple of the diameter of the fluid molecule, σ_{ff}) and a parameter α that measures the ratio of the fluid-wall to the fluid-fluid attractive interaction. Experimental results are also presented for a variety of adsorbates in activated carbon fibers (ACF) covering a wide range of α values; the ACF have slit-shaped pores with average pore width 1.4 nm. The experimental and simulation results show good agreement.

1. Introduction

Numerous experimental studies have been reported for freezing of fluids in pores (for a review, see ref. [1]. Most of the studies using silica-based porous materials show a depression of the freezing temperature when compared with the bulk ($\Delta T_f = T_{f,pore} - T_{f,bulk} < 0$). The possibility of an elevation in freezing temperature was investigated in a simulation study that looked at the effect of confinement on freezing of simple fluids in slit pores by Miyahara and Gubbins [2]. Miyahara and Gubbins studied freezing of Lennard-Jones (LJ) methane in slit-shaped pores with different degrees of the strength of pore-wall interaction. The authors defined "*attractive pores*" as those for which the potential energy of interaction of the pore wall with the confined fluid is *more attractive* than the potential energy of interaction that would result if the pore-wall were to be made up of a solid phase of the fluid molecules that are confined; "*repulsive pores*" were defined as those in which the inverse is true. Their study found that the hysteresis freezing temperature was *increased* for attractive pores and *lowered* for repulsive pores, relative to the bulk material. The hysteresis freezing temperature, as opposed to the thermodynamic freezing temperature, is defined as the limit of metastability of the liquid phase during freezing. In this paper we present a global perspective for understanding the freezing behavior of fluids in porous media. The central result of our paper is that, for freezing of simple fluids in ordered slit-shaped porous materials, the freezing behavior is governed by the pore width and an energy parameter that determines the relative strength of the fluid-wall interaction to the fluid-fluid interactions. Although many experimental results and a few simulation results that we discuss in this paper have already

been published elsewhere [3-8], we now provide a unified picture of the freezing in confined fluids in terms of global phase diagrams, and report additional simulation results that we performed, in order to construct these phase diagrams.

2. Simulation and Experimental Methods

We performed Grand Canonical Monte Carlo (GCMC) simulations of a fluid adsorbed in slit shaped pores of width H, where H is defined as the perpendicular distance between the planes passing through the nuclei of the first layer of molecules that make up the pore walls of the slit shaped pore. The interaction between the adsorbed fluid molecules is modeled using the Lennard-Jones (12,6) potential. The pore walls are modeled as a continuum of LJ molecules (of density ρ_w) using the"10-4-3" Steele potential [9]. The strength of attraction of the pore walls relative to the fluid-fluid interaction is determined by the parameter $\alpha=\rho_w\varepsilon_{fw}\sigma_{fw}^2\Delta/\varepsilon_{ff}$, where σ and ε are the LJ size and energy well depth parameters, respectively, Δ is the distance between graphene layers, and subscripts f and w represent fluid and wall, respectively [3]. Throughout the study the fluid-fluid interaction was kept fixed and the parameters for the wall potential were varied. Eight different sets of parameters were chosen for the pore wall interaction that ranged from a purely repulsive wall to a strongly attractive wall (α=0 to α=2.14). We used the Landau free energy formalism [4] to calculate the free energies of confined phases. The method relies on the calculation of the Landau free energy as a function of an effective bond orientational order parameter Φ, using GCMC simulations [4]. The Landau free energy, Λ, is defined by,

$$\Lambda[\Phi] = -k_B T \ln(P[\Phi]) + \text{constant} \tag{1}$$

where $P[\Phi]$ is the probability of observing the system having an order parameter value between Φ and $\Phi+\delta\Phi$. The probability distribution function $P[\Phi]$ is calculated in a GCMC simulation as a histogram, with the help of umbrella sampling. The grand free energy Ω is then related to the Landau free energy by

$$\exp(-\beta\Omega) = \int d\Phi \exp(-\beta\Lambda[\Phi]) \tag{2}$$

The grand free energy at a particular temperature can be calculated by numerically integrating equation (2) over the order parameter space. We use a two-dimensional order parameter to characterize the order in each of the molecular layers.

$$\Phi_{6,j} = \left| \frac{1}{N_b} \sum_{k=1}^{N_b} \exp(i6\theta_k) \right| = \left| < \exp(i6\theta_k) >_j \right| \tag{3}$$

$\Phi_{6,j}$ measures the hexagonal bond order within each layer j. Each nearest neighbor bond has a particular orientation in the plane of the given layer, and is described by the polar coordinate θ. The index k runs over the total number of nearest neighbor bonds N_b in layer j. The overall order parameter Φ_6 is an average of the hexagonal order in all the layers. We expect $\Phi_{6,j}=0$ when layer j has the structure of a two-dimensional liquid, $\Phi_{6,j}=1$ in the two dimensional hexagonal crystal phase, and $0<\Phi_{6,j}<1$ in an orientationally ordered layer. The state conditions of phase co-existence were determined by requiring the grand free

energies of the confined phases to be equal. The details of the simulations are described in detail elsewhere [5]. A wide range of freezing behavior was observed as the relative strength of the fluid-wall interaction to the fluid-fluid interaction was varied, i.e., by adjusting the value of the parameter α. Global phase diagrams for two different pore widths, $H^*=H/\sigma_{ff}$ = 7.5 and 3.0, were constructed by spanning the parameter space in α and $T_{f,pore}/T_{f,bulk}$, maintaining a pressure of 1atm. The nature of the confined phases were determined by calculations of the in-plane pair correlation functions for the layers of adsorbed molecules [4,5]. In the case of hexatic phases the structure was confirmed by calculations of the orientational pair correlation function, $G_{6,j}(r)$, for the confined molecular layer j; this is defined as

$$G_{6,j}(r) = \langle \Phi_{6,j}^{*}(0)\, \Phi_{6,j}(r) \rangle \qquad (4)$$

With the exception of the point for cyclohexane in *figure 1*, the experimental results were obtained using differential scanning calorimetry (DSC) and dielectric relaxation spectroscopy (DRS) for different fluids confined in activated carbon fibers (ACF). The details of these experiments were published elsewhere [6,7]. For the polar adsorbates both methods were employed, while for carbon tetrachloride and benzene only DSC was used. While both methods enable the freezing temperatures to be determined, DRS also yields the dielectric relaxation time, which is sensitive to the type of phase considered. For example, crystalline and liquid phases exhibit dielectric relaxation times of the order 10^{-3} and 10^{-9} s, respectively, while hexatic and contact layer phases have relaxation times intermediate between these two limits, usually in the range 10^{-5} to 10^{-7}s [7,8]. The identification of the hexatic phase region in the experimental part of *figure 2* is tentative, and is based on the dielectric relaxation times together with knowledge of the phase diagram for the ideal slit pore from simulation. Experiments were performed on various adsorbates viz., water, nitrobenzene, aniline, methanol, carbon tetrachloride, and benzene confined in activated carbon fibers. The experimental point for cyclohexane in *figure 1* was determined by Klein and Kumacheva [8] using a surface force apparatus.

3. Results and Discussion

A summary of the phase behavior of a Lennard-Jones fluid in slit shaped pores of width H^*=7.5 is given in *figure 1*. When filled, such a pore can hold 7 layers of adsorbate molecules. The reduced freezing temperature of the bulk Lennard-Jones fluid (at 1 atm. pressure) is $T^*=kT/\varepsilon_{ff}$ = 0.682 and is depicted by $T_{f,pore}/T_{f,bulk}$=1, the horizontal "dash-dot-dot-dot" line in *figure 1*. In the case of the confined system, the crystal phase boundary is marked by the circles, below which the crystalline phase is stable. The freezing temperature of the confined phase (given by the solid circles) shifts upwards on confinement for values of α greater than 0.95 (strongly attractive pores), and shifts downwards for values of α less than 0.95 (weakly attractive pores). In *figure 1*, the solid squares represent the freezing temperature of a "partially crystalline phase"; the contact layers (layers adjacent to the pore walls) freeze at a different temperature than the inner layers. For strongly attractive pores, the contact layers freeze at a temperature *higher* than the inner layers, while for weakly attractive walls the contact layers freeze at a temperature *lower* than the inner layers. This leads to the formation of two new phases that we term *contact-crystalline* and *contact-liquid* phases, respectively. The contact-crystalline phase is thermodynamically stable in the region $\alpha > 0.95$, between the squares and the circles. The contact-liquid phase is a stable phase in the region $\alpha < 0.95$, between the squares and the circles, but is not observed for very weakly

attractive pores, $\alpha < \sim 0.3$. For strongly attractive pores, the contact layers undergo a liq hexatic phase transition (shown as solid diamonds), that leads to the formation of ano new phase that we term "*contact-hexatic*". The stable regions of the contact-hexatic ph are between the lines marked by the diamonds and the squares in *figure 1*. The freez temperature of cyclohexane in a mica slit-pore of width $7.5\sigma_{ff}$ measured by Klein Kumacheva is in excellent agreement with our calculated global phase diagram for this p width.

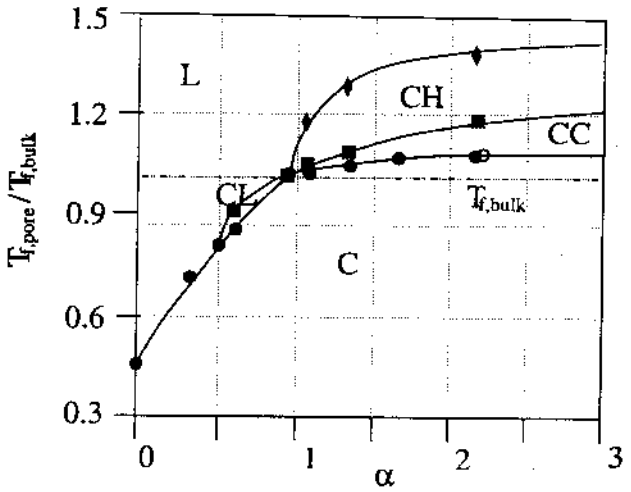

Figure. 1 Global phase diagram for a Lennard-Jones fluid in a slit shaped pore of wi H*=7.5 and a pressure of 1 atm. The symbols specify the conditions of co-existence of t phases, obtained using Landau free energy calculations. The solid lines passing through symbols are a guide to the eye and represent the phase boundaries separating the differ phases. Five different phases are observed: liquid (L), contact-hexatic (CH), contact-crys (CC), contact-liquid (CL) and crystal (C). The open circle represents the only experimen result that we are aware of, for this choice of pore width. This experiment was for freezing seven confined layers of cyclohexane between mica surfaces performed in a surface fo apparatus by Klein and Kumacheva [8].

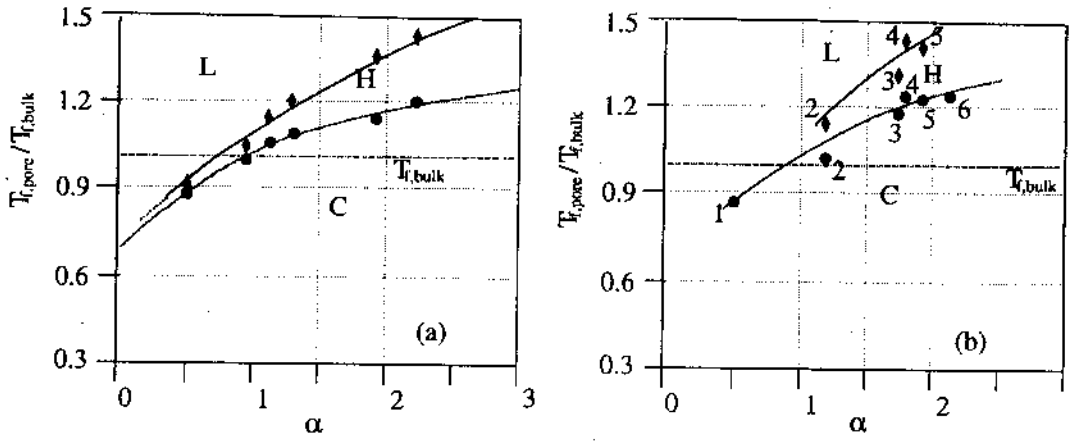

Figure 2. Global phase diagram of a fluid in a slit pore of width H*=3 (a) from simulations, (from experiment. The experiments are for various adsorbates confined within activated carbon fibe (ACF, mean pore width 1.4 nm). Three different phases are observed: liquid (L), hexatic (H), a

crystal (C).The points marked 1-6 correspond to different experimental systems: 1. water in ACF, 2. nitrobenzene in ACF, 3. aniline in ACF, 4. methanol in ACF, 5. carbon tetrachloride in ACF, 6. benzene in ACF.

The global phase diagram for a smaller pore width (H^*=3) is shown in *figure 2* (a), (b). Such pores can hold at most two layers of adsorbate molecules. Thus, for this choice of pore width both layers are contact layers and there are no inner adsorbed layers. Thus "contact layer" phases of the type observed for the larger pore widths cannot occur. The phase boundaries from the simulations and experiments for this system seem to be in generally good agreement (to within 12 % in $T_{f,pore}/T_{f,bulk}$) over the range studied. We note that the mean pore width of the carbon used is 1.4 nm, and because of variations in the diameter of the fluid molecules studied the reduced pore width, H*, varies somewhat among these systems. However, it is approximately 3 for these systems.

This work was supported by grants from the National Science Foundation (Grant No. CTS 9908535) and the U.S.-Poland Maria Sklodowska-Curie Joint fund (grant no. MEN/DOE-97-314). Supercomputer time was provided under a NSF/NRAC grant (MCA93S011).

References

[1] L.D.Gelb, K.E.Gubbins, R.Radhakrishnan, and M.Sliwinska-Bartkowiak, Rep. Prog. Phys. **62** (1999), 1573.
[2] M.Miyahara and K.E.Gubbins, J. Chem. Phys. **106** (1997) 2865.
[3] R. Radhakrishnan, K.E. Gubbins and M. Sliwinska-Bartkowiak, J. Chem. Phys. **112** (2000) 11048.
[4] R.Radhakrishnan and K.E. Gubbins, Mol. Phys. **96** (1999) 1249.
[5] R. Radhakrishnan, K.E. Gubbins, M. Sliwinska-Bartkowiak, J. Chem. Phys. **in press** (2001).
[6] M. Sliwinska-Bartkowiak, G. Dudziak, R. Sikorski, R. Gras, R. Radhakrishnan and K.E. Gubbins, J. Chem. Phys. **114** (2001) 950.
[7] M. Sliwinska-Bartkowiak, G. Dudziak, R. Sikorski, R. Gras, K.E. Gubbins and R. Radhakrishnan, Phys. Chem. Chem. Phys. **3** (2001) 1179.
[8] J. Klein and E. Kumacheva, Science **269** (1995), 816.
[9] W.A.Steele, Surf. Sci. **36** (1973) 317.